

# **Studies of Proteins Using Spectroscopic Approaches**

Prepared by Justina Mary Chinwong  
Dr. Ruel Z. B. Desamero, Mentor

*Chemistry/Honors Program Thesis  
Chemistry/ Natural Sciences Department  
York College: City University of New York*

## Table of Contents

I.	Introduction.....	4
II.	Chapter 1.....	4
	1. Ultraviolet-visible Spectroscopy.....	4
	2. Fluorescence Spectroscopy.....	5
	3. Fourier-Transform Infrared Spectroscopy.....	6
III.	Chapter 2.....	8
	1. Abstract.....	8
	2. Introduction.....	8
	3. Methods and Material.....	8
	4. Results.....	9
	5. Discussion and Conclusion.....	10
IV.	Chapter 3.....	11
	1. Abstract.....	11
	2. Introduction.....	11
	3. Methods and Material.....	14
	4. Results.....	14
	5. Discussion and Conclusion.....	15
V.	Chapter 4.....	15
	1. Abstract.....	15
	2. Introduction.....	16
	3. Methods and Material.....	18
	4. Results.....	19

5. Discussion and Conclusion.....	22
VI. Discussion and Conclusion.....	23
<i>Acknowledgements</i> .....	23
<i>References</i> .....	24

## Introduction

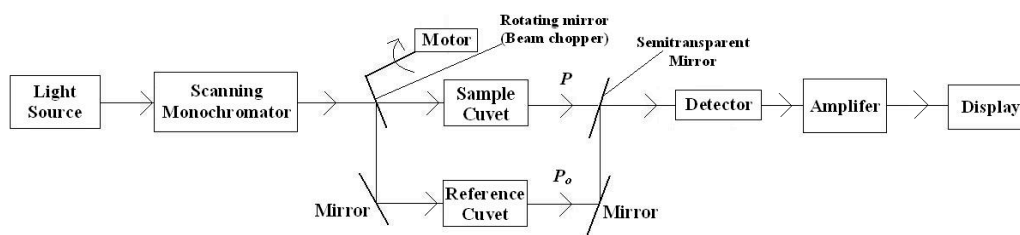
This thesis was written for the Department of Chemistry and the Honors Program at York College of the City University of New York. The studies were performed under the supervision of my mentor, Dr. Ruel Z. B. Desamero. These research projects are concentrated biochemistry. Small molecules are studied using various spectroscopic instruments. By characterizing these molecules, we hope to learn more about their binding processes. We can then use this information to apply it to create therapeutically drugs for different diseases and cancers.

## Chapter 1: Fundamentals of Spectrometry and Spectrometric Instruments

### Ultraviolet-visible Spectroscopy

In an ultraviolet-visible spectrometer, electrons get excited from ground state to an excited state when they absorb the energy from ultraviolet radiation and visible light. Beer-Lambert's Law explains the amount of light absorbed by a sample. The following formula is as follows.  $A = \epsilon bc$ , where  $A$  is absorbance,  $\epsilon$  is a constant that depends on the molecule,  $b$  is the pathlength and  $c$  is the concentration.

The following is a block diagram for a typical UV-visible spectrometer.



Block Diagram of Ultraviolet-visible Spectroscopy  
\*Reproduce with Paint Software

As shown in the diagram, this instrument is composed of many parts. The light source is usually a deuterium lamp which emits electromagnetic radiation in the UV region of the spectrum.

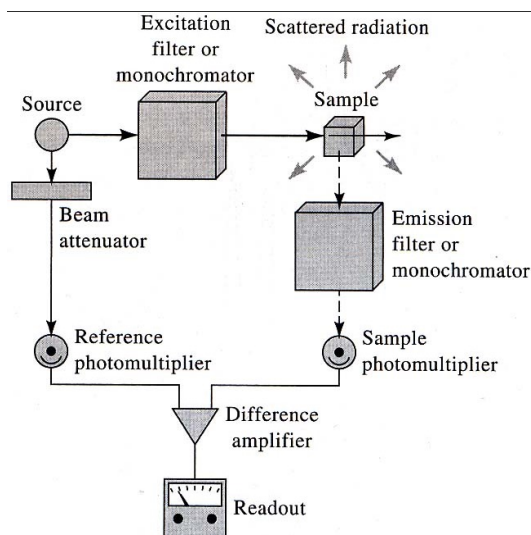
There is usually another source of light called the tungsten lamp. This lamp is used for

wavelengths in the visible region of the spectrum. The light from the light source is split into two beams known as the sample beam and the reference beam. Next, the monochromator is used to spread the beam of light, allowing only the desired wavelength to be shined on the sample and reference cuvet. Some light is absorbed by the sample. However, the light that is not absorbed passes through the sample and reaches the detector. This records the intensity of the transmitted light.

### **Fluorescence Spectroscopy**

In luminescence, molecules can absorb and emit light when they are excited by certain wavelengths. Fluorescence is an example of a luminescence. In fluorescence, electrons get excited via a  $S_0 \rightarrow S_1$  transition path. This means that an electron will go from singlet ground state to its singlet first excited state when excited.

A fluorescence spectrometer gives two different spectra called the emission and the excitation spectra. Emission is also known as the secondary monochromator. It usually gives peaks that are mirror images of the absorption spectra. Moreover, the peaks are observed at lower energy than the absorption spectra. During emission, the excitation wavelength is held constant and the emission wavelength varies. The excitation spectrum is also known as the primary monochromator. Excitation gives a spectrum that looks almost identical to an absorption spectrum. The emission wavelength is constant and the excitation wavelength is variable. The following illustrates a block diagram of a typical fluorescence spectrometer. This source was borrowed from my CHEM341: Instrumental Analysis lecture handouts on fluorescence.



**Block Diagram of a Fluorescence Spectrometer**

**\*\*Figure borrowed from CHEM 341 Fluorescence lecture handouts**

As depicted above, a typical fluorescence spectrometer is composed of excitation and emission monochromators. The excitation monochromator is usually perpendicular to the emission monochromator. As the source is passed through the monochromator and hits the sample, light is scattered in all directions and detected.

### **Fourier-Transform Infrared Spectroscopy**

In Fourier-Transform infrared (FTIR) spectroscopy, changes in dipole moments is measured in molecules. A series of vibrations is caused when infrared is shined on the sample. Furthermore, in order for the sample to absorb and give off vibrational modes, it must be composed of molecules with the same frequency as that of infrared. Moreover, these vibrational modes can then be detected on a spectrum.

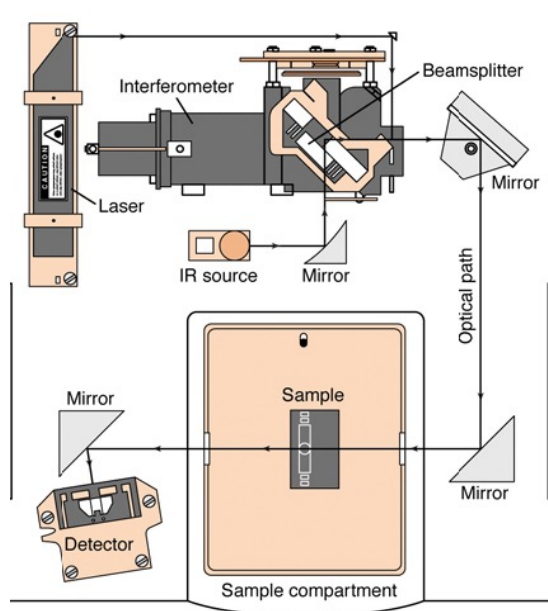
A way to verify the results obtained using FTIR, Hooke's Law may be used to determine the frequency of a molecule. The follow is the formula was proposed for finding the frequency of different molecules.

$$\nu = (1 \div 2\pi) \sqrt{k \div \mu} \quad \text{Where } \mu = (m_1 m_2) \div m_1 + m_2$$

### Equation 1: Hooke's Law

In the above equation, k is the force constant, m1 and m2 are the masses of different atoms,  $\mu$  is the reduced mass and  $\nu$  is the frequency of a molecule one wishes to find. The value for frequency will depend on how heavy the atoms and how strong the bonds are. Another important factor is the units in which these things are measured in. The most important is frequency, and it is measured in  $\text{cm}^{-1}$ . Moreover, as for the spectra range, chemists are most interested in finding peaks ranging from  $650\text{-}2000 \text{ cm}^{-1}$ .

The following is a block diagram of the instrument used in the lab obtained from CHEM341: Instrumental Analysis lab handout.



**Block Diagram of an FTIR instrument**

**\*\*Source borrowed from lecture handout on FTIR**

As shown, before hitting the sample, the FTIR source goes through a series of mirrors. The interferometer, in place of a chromatographer, creates a combination of sine and cosine functions and transforms them into plots. The detector then detects this signal to give spectra.

## **Chapter 2: Spectroscopic Studies of 6, 7-dimethyl-5,6,7,8-tetrahydropterine (DMTHP)**

### *Abstract*

Time and temperature dependent stability studies were performed with UV-vis spectroscopy on 6,7-dimethyl-5,6,7,8-tetrahydropterine (DMTHP), an potential inhibitor of DHPR. Our results suggest that DMTHP is not stable at 44° C. Its wavelength shifts from 300 to 320 nm in less than 20 minutes. Moreover, our studies show that it is stable at 4° C, with a  $\lambda_{\max}$  at 300 nm for more than one hour. From these results, we can conclude that future studies experimented with DMTHP have to be done at 4° C.

### **Introduction**

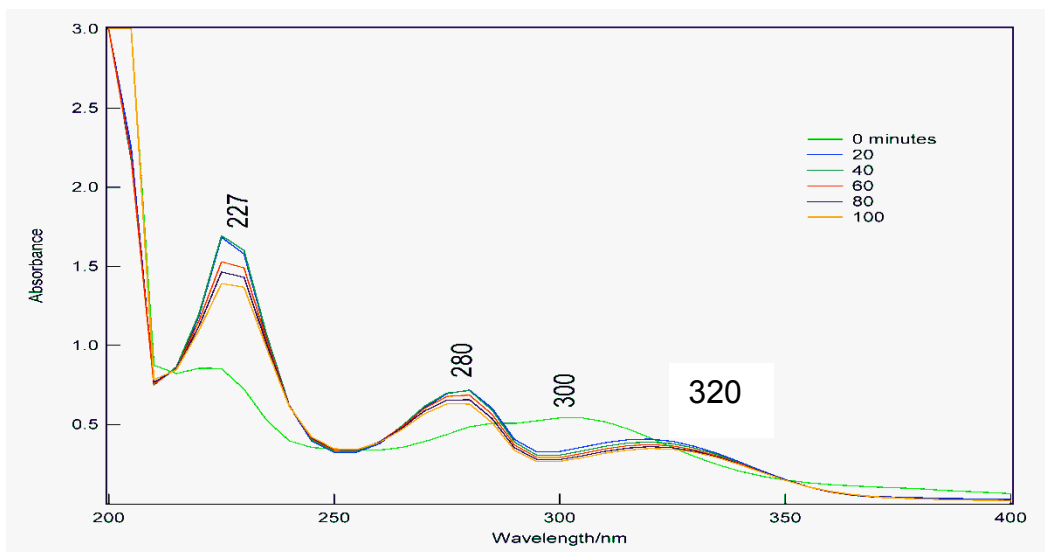
DMTHP is a potential inhibitor of a protein called dihydropteridine reductase (DHPR) (discussed further in chapter 3). Before we studied the interactions between DMTHP and DHPR, we determined the stability of DMTHP. These stability studies were important because they act as the control for our experiments. We were able to determine whether changes in peak positions and intensities were from interactions between the protein and its inhibitor or whether they were from the inhibitor alone.

### **Methods and Materials**

***Samples*** Solutions of 50 $\mu$ M DMTHP in 50 mM Tris-HCl buffer in deionized water were prepared.

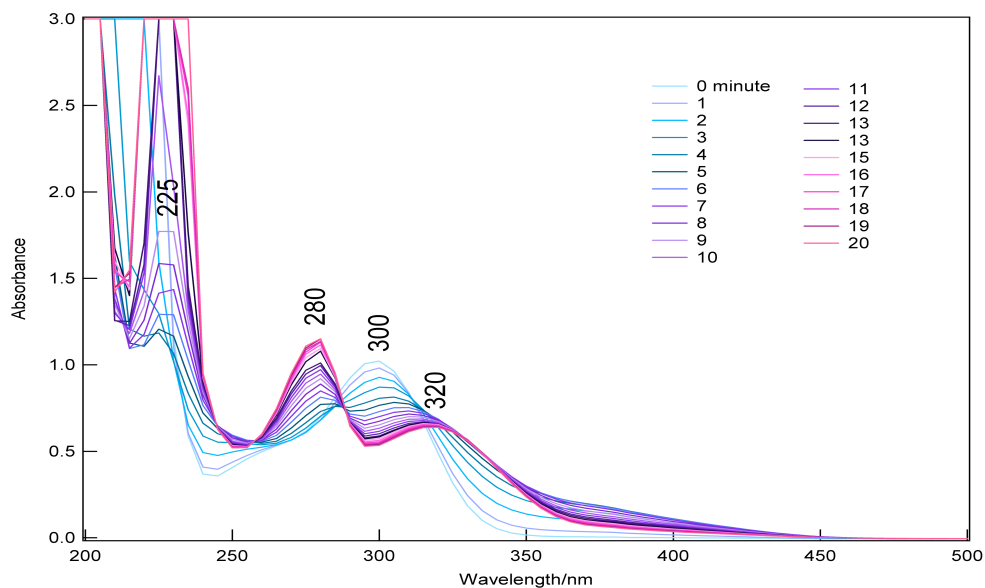
***UV-vis Spectroscopy*** The model used was Perkin Elmer, Lamda 25 UV-vis spectrometer. The temperatures used for each run were 44, 24 and 4° C. 1 nm data intervals were used.

## Results



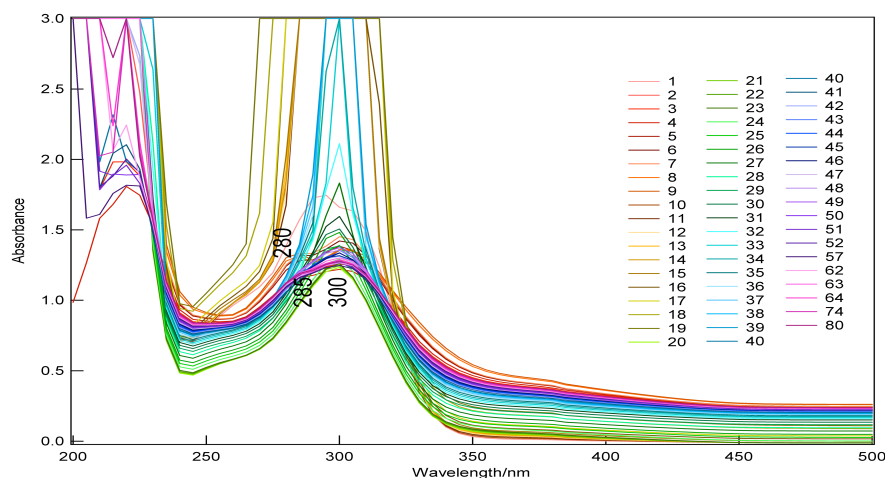
**Figure 1: DMTHP at 44° C**

Figure 1 shows 6 spectra of 50 μM DMTHP at 44° C, with 20 minutes intervals between each run. As evident, within 20 minutes the absorbance peak at 300 nm shifted to 320 nm, and the absorbance peaks at 227 and 280 nm increased in intensities.



**Figure 2: DMTHP at 44° C with 1 minute time intervals**

Figure 2 shows the spectra for DMTHP at 44° C each minute in a 20 minute time period. As shown, at 0 minute, the absorbance peaks are at 225 and 300 nm. The absorbance peak at 225 nm drastically varied in absorbance intensity within this time period. In about 5 minutes, an absorbance peak at 280 nm appeared, and the absorbance peak at 300 nm shifted to about 320 nm.



**Figure 3: DMTHP in 4° C**

Figure 3 demonstrates the UV-vis spectra of 50  $\mu$ M DMTHP at 4° C. Evidently, within the first 20 minutes, there are three peaks at 225, 280 and 300 nm. However, after 80 minutes, we see one peak at 300 nm and a shoulder peak at 285 nm.

### **Discussion and Conclusion**

Our results indicate that DMTHP is not stable at 44° C. This conclusion is deferred from Figures 1 and 2 that show the peak at 300 nm shifts to 320 nm. This result is chemically significant because we know that a shift of 18 nanometers is an indication of an alkyl group or a ring residue on the  $\gamma$  carbon or a carbon of higher number. Therefore, our results may imply that at 44° C, the structure of DMTHP has been chemically modified in the former fashion.

We can conclude that DMTHP cannot be studied at 44° C because of drastic shifts in wavenumbers and absorbance intensities. However, there is very little, if any, wavenumber shifts in DMTHP at 4° C. Therefore, as a conclusion from these results, we may perform further studies with this molecule at 4° C. It has a  $\lambda_{\text{max}}$  at 300 nm. In future studies (as discussed in the next chapter), we use this absorbance peak to determine interactions between this inhibitor and DHPR.

### **Chapter 3: Spectroscopic Analysis of DHPR, DMTHP and NADH**

#### *Abstract*

Dihydropteridine reductase (DHPR) is important enzyme in the brain. When there is a deficiency in this enzyme, a type of neurological disease known as phenylketonuria (PKU) can occur. In this research experiment, we study potential inhibitors of DHPR in order to better understand how src kinase works. The inhibitor used was 6, 7-dimethyl-5,6,7,8-tetrahydropterine (DMTHP). We were able to determine that there are interactions between DHPR, its cofactor, and DMTHP are studied using fluorescence spectroscopy.

#### **Introduction**

Dihydropteridine reductase (DHPR) is an important enzyme in the brain that uses NADH as a cofactor for recycling 5,6,7,8-tetrahydrobiopterin ( $\text{BH}_4$ ) from quinonoid dihydrobiopterin ( $\text{qBH}_4$ ). The following diagram shows this process.

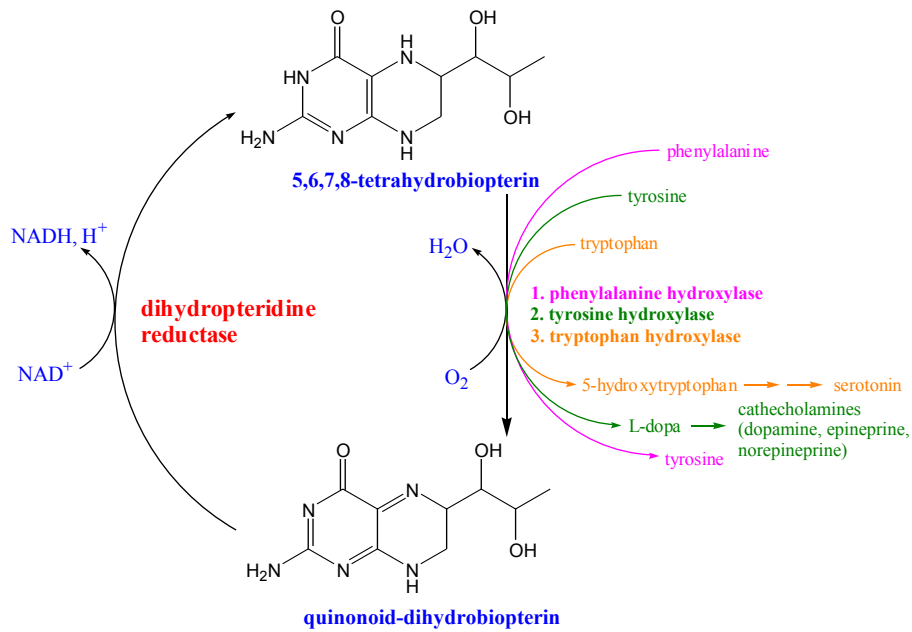


**Figure 1: Biological Mechanism of DHPR**

As stated, recycling of qBH<sub>4</sub> is essential because it converts into BH<sub>4</sub>. BH<sub>4</sub> is needed for other biological processes such as biosynthetic reactions of phenylalanine, tyrosine, and tryptophan. A deficiency in DHPR does not allow proper recycling of qBH<sub>4</sub>. When this occurs, it results in improper function of enzymes such as phenylalanine hydroxylase. As consequence, phenylalanine does not get converted to tyrosine and builds up in the brain. Hence, this type of DHPR deficiency can lead to a neurological disease known as phenylketonuria (PKU).

In recent studies, the crystal structure of DHPR and its cofactor was determined. Figure 2 illustrates the crystal structure of DHPR and its cofactor NADH.

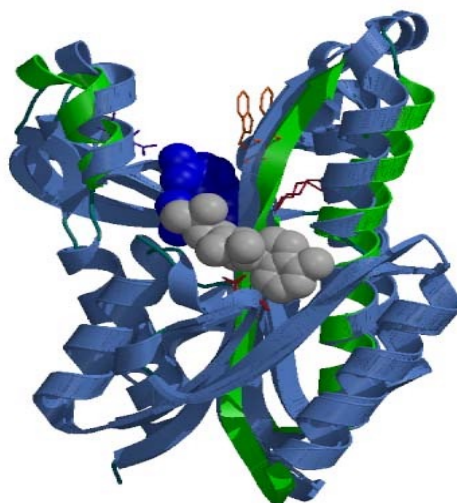


**Figure 2: X-ray Crystal Structure of DHPR and NADH**

The apo form of DHPR is indicated by the blue ribbons. DHPR domains shift upon NADH (shown in the center of the protein in CPK) binding as indicated by the green ribbons. Even though the crystal structure for the holoenzyme has been determined, its crystal structure with its ligand,  $\text{BH}_4$ , has not been determined. Therefore, we proposed to use spectroscopic analysis to determine the interactions between this enzyme and its ligands. Furthermore, we use Gaussian 03W simulations to account for our experimental data. The ligand we studied was DMTHP. As discussed in chapter 2, this ligand is an inhibitor of DHPR. It is a good indicator of binding because it is structurally similar to the reactive site in quinonoid-dihydrobiopterin. Figure 3 shows the similarities between DMTHP and  $\text{BH}_4$ .

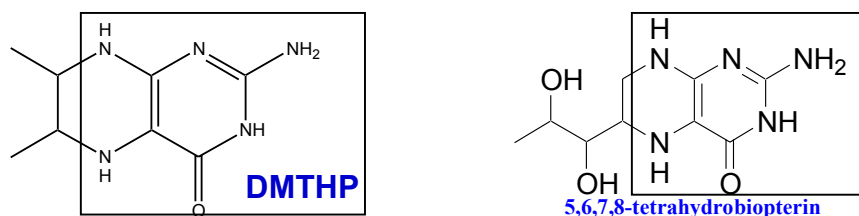


**Figure 3: Chemical Structures of DMTHP and  $\text{BH}_4$**

The structures that are shown in boxes are believed to react with the active site of DHPR. Once incorporated with the enzyme, we expect DMTHP to bind and inhibit further catalytic reactions of DHPR with  $BH_4$ . We propose to study this binding process in order to better understand how DHPR works.

## Material and Methods

**Samples** All samples were prepared in Tris-HCl buffer using deionized water. DHPR was prepared at a concentration of  $4 \mu M$  and its ligands were both prepared at  $8 \mu M$ .

**Fluorescence Spectroscopy** The fluorescence model used was Perkin Elmer, LS-50B. The emission and excitation wavelengths varied according to the  $\lambda_{max}$  obtained for each compound, with slits of 2.5 nm for both primary and secondary monochromators.

## Results

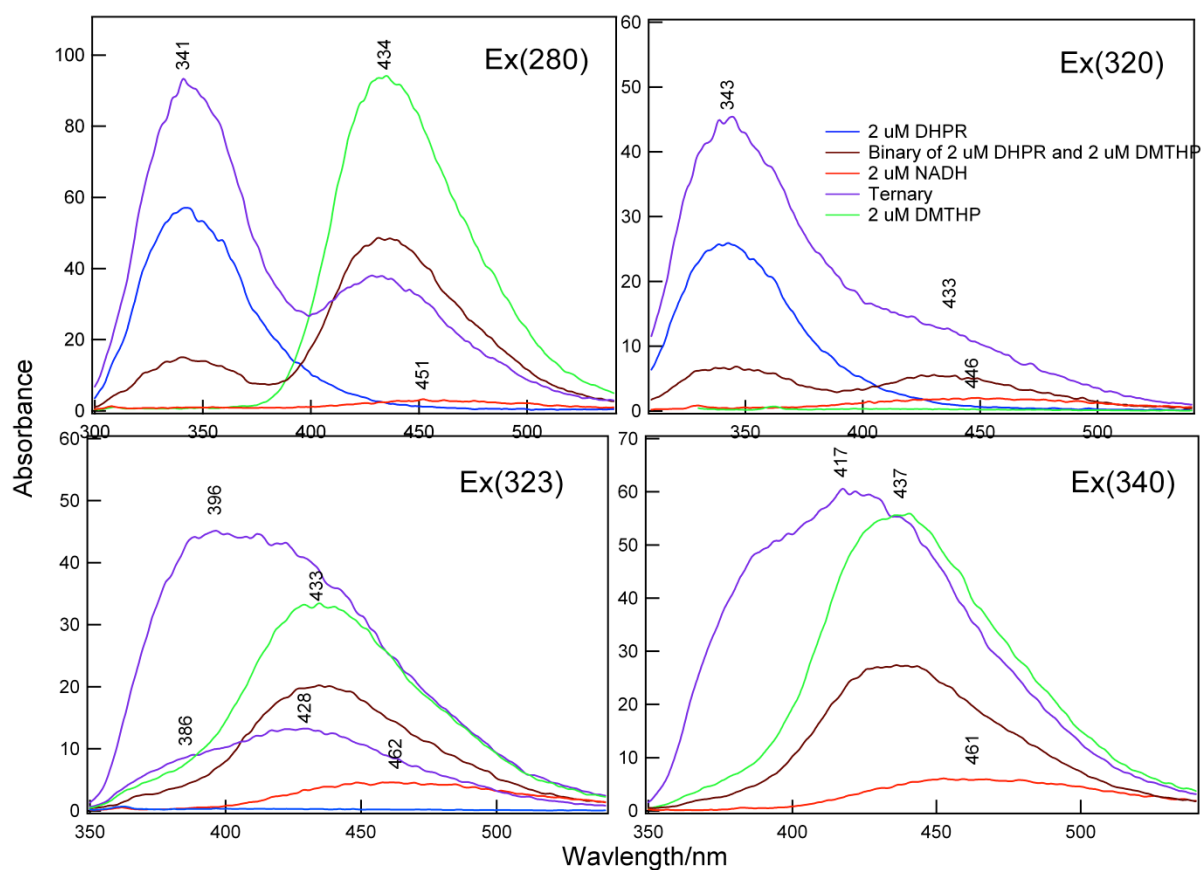


## **Figure 4: Fluorescence Spectra of Single Molecules, Binaries, and Ternary Systems Excited at Different Wavelengths**

Figure 4 illustrates the fluorescence spectra for 2 uM DHPR, 2 uM DMTHP, 2 uM NADH, the binary system of 2 uM DHPR and 2 uM DMTHP, and a ternary system of DMTHP, NADH, and DMTHP.

### **Discussion and Conclusion**

Our results suggest that there are interactions between DHPR and its ligands. When excited at the DMTHP peak (323 nm) and the NADH peak (340 nm), the emission peak for the ternary system has a higher quantum yield than that of the binary system. Moreover, its peak becomes broader than the molecules when they are excited alone. The fact that the quantum yield of the ternary system increases more than two times the quantum yield of the binary system tells us that the system consists of higher energy. Moreover, we confirm that the ternary system consists of higher energy because its peak broadens and becomes slightly blue-shifted. We can conclude from these results that there is an energy transfer between the molecules when placed in a ternary system. Note that the molecules must be in a ternary system in order to observe this increase in quantum yield and energy.

## **Chapter 4: Fourier-Transform Infrared Analysis of Some Amino Acids that are Precursors of Bivalent Src Kinase Inhibitor**

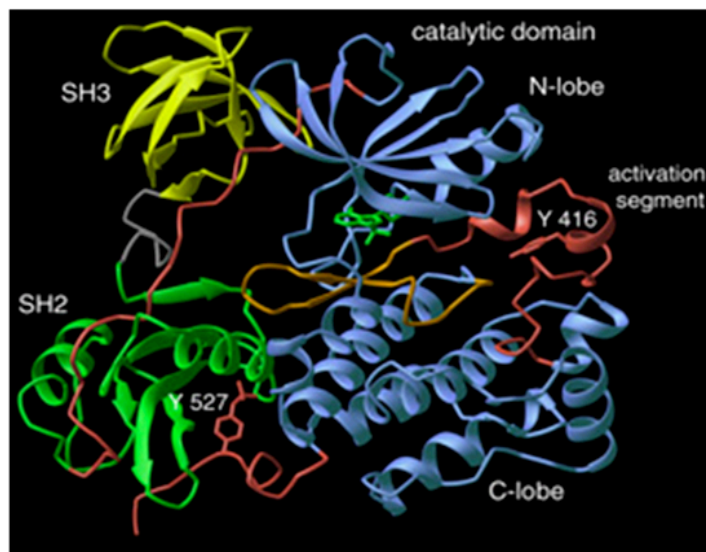
### ***Abstract***

Src kinases are important enzymes that phosphorylate proteins involved in different biological mechanisms. Mutated src kinase continuously phosphorylates these proteins and as a result has shown to lead to cancer in animals. Our ultimate goal is to study how src kinase interacts with synthetically modified bivalent inhibitors. However, before we can do this, we

obtained marker bands that would be good indicators of binding. These markers bands include the aromatic group in pentafluorophenylalanine and the phosphate group in phosphotyrosine. In this experiment, marker bands were found using Fourier-Transform Infrared (FTIR) spectroscopy. We verified our experimental results and found the vibrational modes for these peaks using Gaussian 03W simulations.

## Introduction

Src kinase is an enzyme that belongs to a family of proteins called the tyrosine kinases. It was the first of its kind to be discovered. These proteins are important for many biological processes such as cell signaling, proliferation and survival. Their main role is to catalyze the phosphorylation from ATP to a tyrosine amino acid on different targeted proteins. Figure 1 illustrates the crystal structure of Src Kinase.

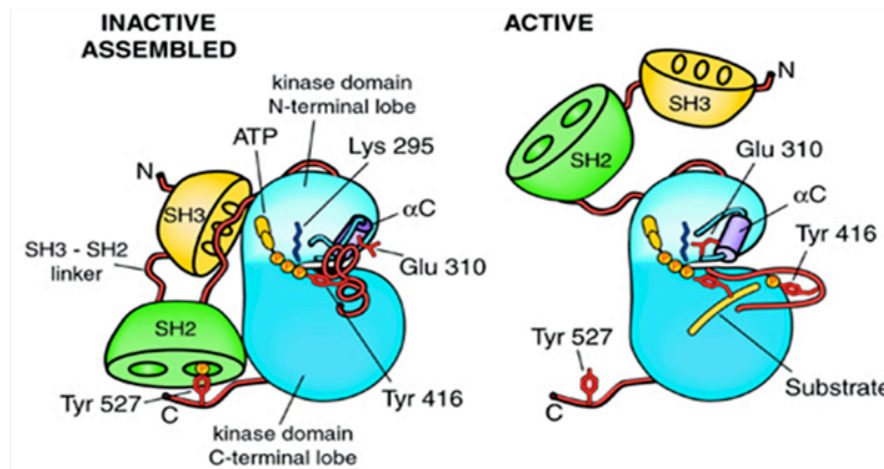


Picture obtained from: <http://jkweb.mcb.berkeley.edu/>

**Figure 1: Crystal Structure of Src Kinase**

It is composed of 451 amino acids and 3 domains. We are interested at the SH2 and catalytic domains which can be seen in Figure 1. The SH2 domain recognizes phosphotyrosine residues

that are important for cell signaling. Moreover, the phosphotyrosine residue pTyr 527 on the C-terminal of the catalytic domain is important for inhibiting the active form of src kinase. It is believed that Tyr 527 acts like an inhibitor once binded to the SH2 domain, giving the inactive form of src kinase. Figure 2 shows the regulation of src kinase upon phosphorylation and dephosphorylation.



[http://jkweb.mcb.berkeley.edu/external/research-in-progress/5-3/signaling/src\\_kinases.html](http://jkweb.mcb.berkeley.edu/external/research-in-progress/5-3/signaling/src_kinases.html)

**Figure 2: Regulation of Src Kinase**

As further shown, the active form of src kinase is when the SH2 domain is free and not binded to Tyr 527. However, the exact mechanism of how this occurs is not yet known. Therefore, it leads to interesting research proposals.

Mutated src kinases are missing tyrosine 527. Therefore, they are continuously active and continuously phosphorylate various proteins. In animals, this mutation results leads to several types of cancers such as colon and breast cancer. Many types of artificially synthesized inhibitors have been reported that bind to mutated src kinase. These inhibitors are usually bivalent and include a phosphotyrosine on one end and a pentafluorophenylalanine on the other end. Moreover, one end binds to the SH2 site and the other to the catalytic domain. Dr. Adam

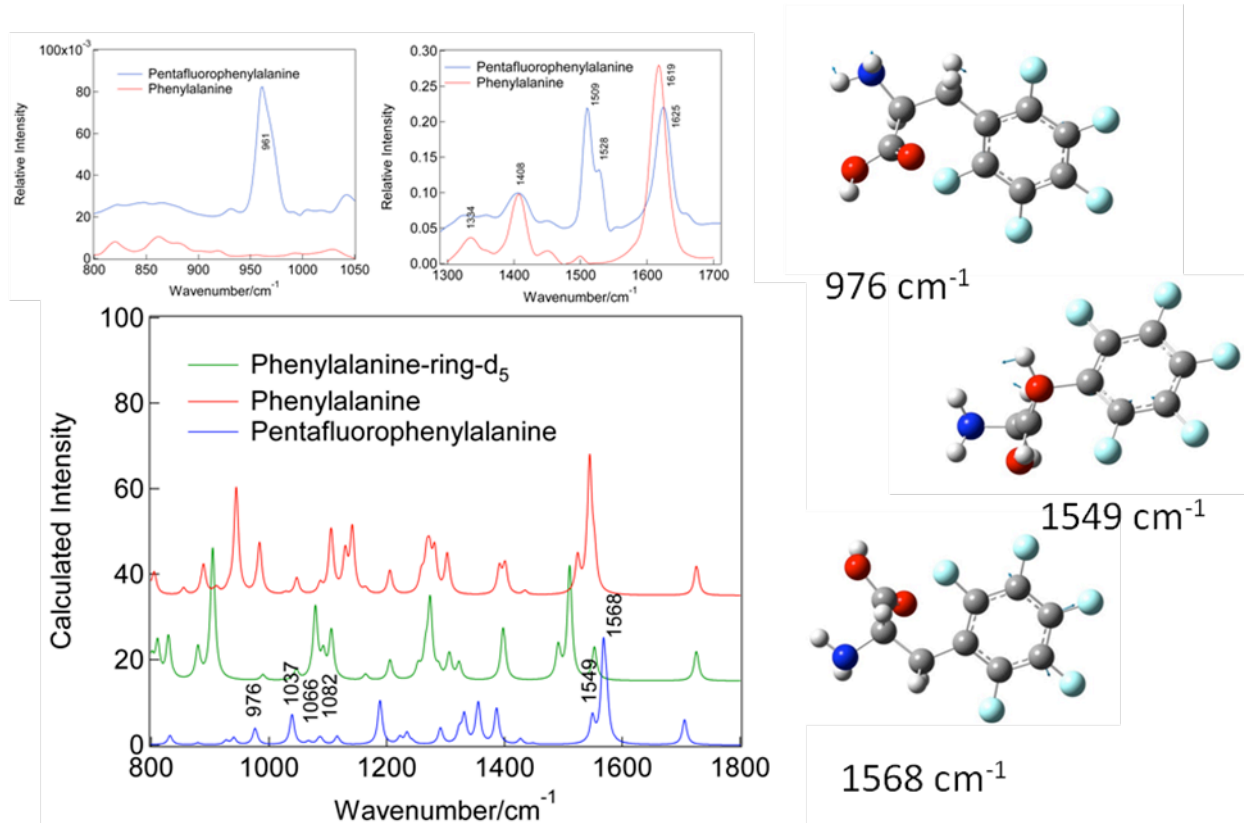
Profit and his lab members have synthesized a bivalent inhibitor with these characteristics. The ultimate goal of this experiment is to see how this inhibitor binds to src kinase. However, first we identify marker bands that are potential indicators of binding by examining the amino acids synthetically incorporated into the bivalent inhibitor. We believe that the phosphate and aromatic functional groups in phosphotyrosine and pentafluorophenylalanine, respectively, are involved in the binding process. Therefore, we identify the positions of these markers bands by comparing these amino acids to their derivatives tyrosine and phenylalanine, respectively. Once these markers bands are identified, we hope to see them when the bivalent inhibitor is studied, and track any changes when incorporated with the enzyme.

## **Material and Methods**

***Fourier Transform Infrared Spectroscopy*** The model of FTIR used was Nicolet Nexus, 670 FT-IR. All the compounds under study were scanned 128 times at a resolution of 8, which corresponds to a data spacing of  $3.857\text{ cm}^{-1}$ . AgCl, NaCl, and CaF<sub>2</sub> windows and a spacer of 0.025 mm were used. The buffers were prepared using D<sub>2</sub>O as solvent.

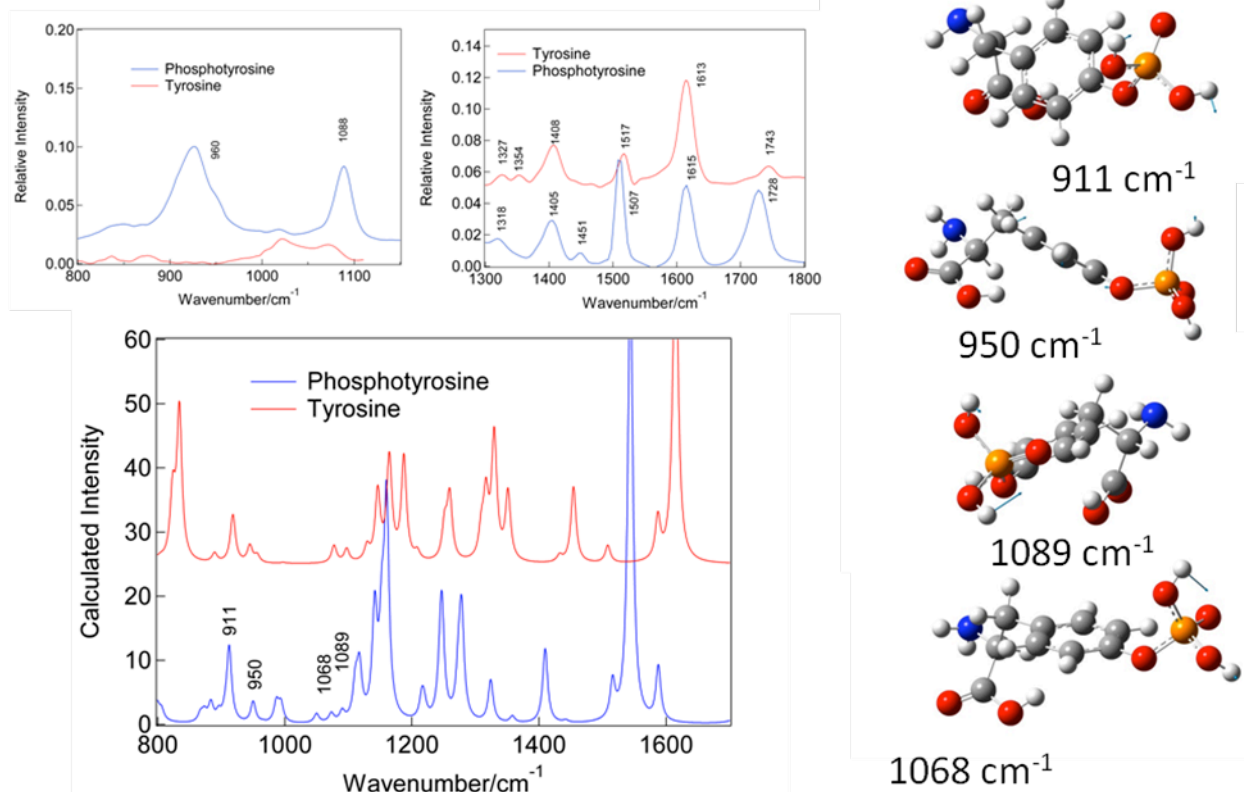
***Gaussian 03W Computer Software*** Gaussian 03W was used to perform calculations for phenylalanine, phenylalanine-ring-d<sub>5</sub>, pentafluorophenylalanine, tyrosine, and phosphotyrosine. We ran an optimization followed by frequency calculations using the method DFT with B3LYP and basis set 6-31g (d).

## Results



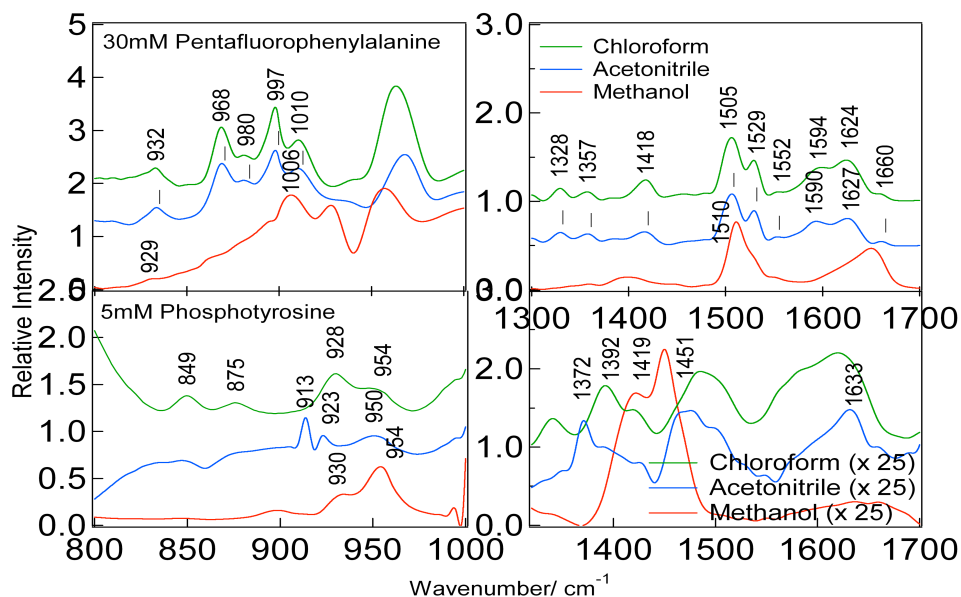
**Figure 3: FTIR Experimental and Theoretical Spectra and FTIR Vibrational Modes for Pentafluorophenylalanine**

Figure 3 shows the experimental FTIR spectra (two spectra above) for pentafluorophenylalanine and phenylalanine. Pentafluorophenylalanine has three distinguished experimental peaks at 961, 1509, and 1528  $\text{cm}^{-1}$ . This figure also shows that calculated FTIR spectra (calculated) for phenylalanine-ring- $\text{d}_5$ , phenylalanine, and pentafluorophenylalanine. As shown, pentafluorophenylalanine has distinguished peaks at 976, 1549, and 1568  $\text{cm}^{-1}$ . The vibrational modes for these calculated peaks are illustrated to the right of the figure.



**Figure 4: FTIR Experimental and Theoretical Spectra and FTIR Vibrational Modes for Phosphotyrosine**

Figure 4 shows the experimental FTIR spectra (two spectra above) for phosphotyrosine and tyrosine. Phosphotyrosine has one distinguished experimental peak at  $960\text{ cm}^{-1}$ . Figure 4 also shows that calculated FTIR spectra (calculated) for phosphotyrosine and tyrosine. In particular, phosphotyrosine has two distinguished peak at  $911$  and  $950\text{ cm}^{-1}$ . The vibrational modes for these calculated peaks are illustrated to the right of the figure.



**Figure 5: Solvent Dependence of Amino Acids in FTIR**

Figure 5 shows the spectra for pentafluorophenylalanine and phosphotyrosine in different solvents. The three solvents used were chloroform, acetonitrile, and methanol. The following table (Table 1) shows the wavenumbers for the peaks of both amino acids in different solvents.

**TABLE 1: Marker bands in Different Solvents**

Solvent	D <sub>2</sub> O	Methanol	Acetonitrile	Chloroform
<b>Molecule</b>	<b>Marker Bands (cm<sup>-1</sup>)</b>			
<b>PFP</b>	<b>961</b>	-	<b>968</b>	<b>968</b>
	<b>1509</b>	<b>1518</b>	<b>1505</b>	<b>1505</b>
	<b>1527</b>	-	<b>1529</b>	<b>1529</b>
<b>Ptyr</b>	<b>926</b>	<b>930</b>	<b>913/923</b>	<b>928</b>

As shown, we were able to see the determined marker bands in all compounds except for methanol. The peak at 961 and 1527 cm<sup>-1</sup> are not seen for pentafluorophenylalanine in methanol.

## Discussion and Conclusion

Our results indicate that marker bands were found for pentafluorophenylalanine and phosphotyrosine in D<sub>2</sub>O solvent. The marker bands found for pentafluorophenylalanine were at 961, 1509, and 1527 cm<sup>-1</sup>. The marker bands found phosphotyrosine was at 926 cm<sup>-1</sup>. Next, we will use these marker bands in order to study the bivalent inhibitor. When studying this peptide, we hope to see the marker bands within the same wavenumbers we found for the amino acids studied.

After determining experimental marker bands for pentafluorophenylalanine and phosphotyrosine in D<sub>2</sub>O, we verified these results with theoretical calculations with the computer software Gaussian 03W. In order to verify that these peaks belonged to the aromatic and phosphate functional groups, we obtained their vibrational modes by using also using Gaussian 03W. As was shown, we were able to conclude that the marker bands determined are belong to the functional groups of interest. These results indicate that they are good indicators of binding.

We also ran some solvent dependence measurements of pentafluorophenylalanine and phosphotyrosine. We observed most of our marker bands in the three solvents used, except for methanol. The peak at 961 cm<sup>-1</sup> for pentafluorophenylalanine cannot be seen in this solvent. This observation is due to the fact that methanol has an –OH functional group that blocks the spectrum in this region. These results are significant because it tells us that we can use these marker bands in order to study the bivalent inhibitor *in vivo*. The protein environment very different from the environments the amino acids were exposed to. We purposely used three solvents with varying polarities. Chloroform is the least polar solvent, followed by acetonitrile, and methanol is the most polar. We can make predictions about how the marker bands will vary by using solvents this range in polarity.

## **Discussion and Conclusion**

Our findings in these studies are significant in different ways. Discovering the DMTHP is unstable under high temperatures let us prepare our DHPR studies accordingly. These precautions eliminated possibilities for unreal results. Our DHPR studies determined that there are interactions between DHPR and its ligands. Fourier-Transform Infrared can be used to study what bonds are involved in these interactions. This spectroscopic machine was the basis for our Src kinase study. We determined marker bands for pentafluorophenylalanine and phosphotyrosine. These marker bands set the ground for possible future experiments studying the bivalent Src kinase inhibitor and its interactions with Src kinase. Hopefully, these research findings can be used help understands the proteins DHPR and Src kinase better.

## **Acknowledgments**

I would like to thank my mentor, Dr. Ruel Z. B. Desamero for his guidance and support since I started research in Fall 2005. I would also like to thank New York City Louis-Stokes Alliance for Minority Participation (NYC-LSAMP) for helping to fund my undergraduate research work. Moreover, I would like to thank the lab members who have helped make my undergraduate research experience more plausible and the Chemistry Department for helping me with subtle theories in the sciences.

## References

The Src Kinases. Retrieved January 8, 2007, from Kuriyan Lab Web site:

[http://jkweb.berkeley.edu/external/research-in-progress/5-3/signaling/src\\_kinases.html](http://jkweb.berkeley.edu/external/research-in-progress/5-3/signaling/src_kinases.html)